Parameter estimation in IMEX-trigonometrically fitted methods for the numerical solution of reaction-diffusion problems

Raffaele D'Ambrosio[1], Martina Moccaldi[2], Beatrice Paternoster[2]

[1] *Department of Engineering and Computer Science and Mathematics, University of L'Aquila, e-mail: raffaele.dambrosio@univaq.it*
[2] *Department of Mathematics, University of Salerno, e-mail: {mmoccaldi,beapat}@unisa.it*

Abstract

In this paper, an adapted numerical scheme for reaction-diffusion problems generating periodic wavefronts is introduced. Adapted numerical methods for such evolutionary problems are specially tuned to follow prescribed qualitative behaviors of the solutions, making the numerical scheme more accurate and efficient as compared with traditional schemes already known in the literature. Adaptation through the so-called *exponential fitting technique* leads to methods whose coefficients depend on unknown parameters related to the dynamics and aimed to be numerically computed. Here we propose a strategy for a cheap and accurate estimation of such parameters, which consists essentially in minimizing the leading term of the local truncation error whose expression is provided in a rigorous accuracy analysis. In particular, the presented estimation technique has been applied to a numerical scheme based on combining an adapted finite difference discretization in space with an implicit-explicit time discretization. Numerical experiments confirming the effectiveness of the approach are also provided.

Keywords: Reaction-diffusion problems, periodic plane wave solutions, trigonometrical fitting, parameter estimation, adapted method of lines, IMEX methods.

1. Introduction

The work is focused on the numerical solution of nonlinear reaction-diffusion problems

$$\frac{\partial u}{\partial t} = d_1 \frac{\partial^2 u}{\partial x^2} + f_1(u, v),$$
$$\frac{\partial v}{\partial t} = d_2 \frac{\partial^2 v}{\partial x^2} + f_2(u, v), \tag{1.1}$$

where $d_1 > 0$ and $d_2 > 0$ are the diffusion coefficients and $u, v : [0, \infty) \times [0, T] \longrightarrow \mathbb{R}$ are state variables denoting, for example, the concentrations of two interacting biological species. The nonlinearity in the reaction term $[f_1(u, v), f_2(u, v)]^\intercal$ is generally due to the

occurrence of feedbacks, whereby a component influences (positively or negatively) its evolution or the evolution of the other constituents.

These problems are widely used in applications involving oscillatory dynamical systems (compare, for instance, [14, 15, 25, 26, 27, 28, 29, 30] and references therein), because their dynamics is typically characterized by the generation of wavefronts [19]. Hence, since the main feature of these systems is the wave behavior of their fundamental solutions, it is worth assessing numerical schemes which accurately reproduce it in the discretized dynamics. In particular, we aim to overcome a classic gap of standard numerical methods for oscillatory evolutionary problems, i.e. their requirement of employing a very small stepsize to accurately reproduce an oscillatory dynamics, due to the fact that they are thought as *general purpose* formulae developed in order to be exact (within round-off error) on polynomials up to a certain degree. When the exact solution of a problem has a particular a-priori known behavior (e.g. periodic, oscillatory in time and space, exponentially decaying), it may be more convenient to use fitted formulae that are exact on functions other than polynomials: this technique is nowadays well-known as *exponential fitting* (see [18, 20] and references therein) and the chosen basis functions are normally assumed to belong to a finite-dimensional space called *fitting space*. The fitting space is selected according to the a-priori known information about the exact solution and, as a direct consequence of this choice, the basis functions also depend on parameters related to the solution (e.g. the frequency of the oscillations for oscillatory problems), whose values are clearly unknown.

Briefly, the main challenges connected to a significant use of exponentially fitted methods are the choice of an appropriate fitting space and the accurate estimate of the unknown parameters. This paper focuses on this last problem, by proposing an estimation strategy based on minimizing the leading term of the local truncation error.

The numerical scheme presented here is obtained extending the ideas introduced in [11] for λ-ω systems to a general reaction-diffusion system (1.1): it consists in a spatial discretization of the (1.1) through trigonometrically fitted finite differences and the time integration of the resulting system of ordinary differential equations, having the expression

$$y' = Ay + f(y),$$

where A is a matrix whose size depends on the number of spatial grid points and $f(y)$ is a vector-valued function. We focus on systems having a stiff component (arising from the diffusion term) and a relatively nonstiff one (coming from the reaction term).

Due to this mixed nature, we follow the path drawn in the existing literature (see, for instance, [1, 2, 3, 4, 21, 31] and references therein) by using an implicit-explicit (IMEX) numerical method that implicitly integrates the stiff terms and explicitly integrates the other ones. For the numerical integration of the system, a totally explicit method would require strong restrictions on the stepsize in order to guarantee the stability because of the stiffness. On the other side, a fully implicit method would better treat the stiffness but would be more expensive than an explicit one in order to accurately handle the nonlinearity. Hence, it may be convenient to use IMEX methods because they implicitly integrate only the components that need it (stiff constituents) and explicitly integrate the other ones, with benefits in terms of stability and efficiency. Such a benefit, in the context of reaction-diffusion and advection-diffusion problems,

has been highlighted, for instance, in [21, 31] and references therein.

In summary, we develop a problem-oriented numerical scheme for a general reaction-diffusion system, described in Section 2, while Sections 3 and 4 provide an error analysis of the method and propose an estimate of the unknown parameters. Section 5 shows numerical experiments confirming the effectiveness of the approach; finally, Section 6 is devoted to concluding remarks.

2. Adapted numerical scheme

The numerical scheme we propose, extending the ideas in [5, 6, 7, 10, 11, 12], relies on a finite difference spatial discretization of the problem, by means of an adapted method of lines. Thus, as a first necessary step, we need to specify our numerical domain: indeed, the state variables u and v in (1.1) are defined in an unbounded domain, but we numerically integrate the system (1.1) in its bounded counterpart

$$\overline{\mathcal{D}} := [0, X] \times [0, T], \tag{2.2}$$

where X is chosen large enough that any increase would only have negligible effects on the solution. Following the method of lines (see [17, 22, 23] and references therein), we spatially discretize the domain (2.2)

$$\overline{\mathcal{D}}_h = \{(x_i, t) : x_i = i h, i = 0, \ldots, N - 1, h = X/(N - 1)\},$$

where h is the spatial stepsize. Then, the spatially discretized version of (1.1) with initial conditions

$$u(x, 0) = \psi_1(x), \quad v(x, 0) = \psi_2(x), \tag{2.3}$$

and suitable boundary conditions assumes the form

$$u'_0(t) = \zeta_1(t), \tag{2.4a}$$
$$v'_0(t) = \zeta_2(t), \tag{2.4b}$$
$$u'_i(t) = d_1 \Delta_n[u_i(t), h] + f_1(u_i(t), v_i(t)), \quad i = 1, \ldots, N - 2, \tag{2.4c}$$
$$v'_i(t) = d_2 \Delta_n[v_i(t), h] + f_2(u_i(t), v_i(t)), \quad i = 1, \ldots, N - 2, \tag{2.4d}$$
$$u'_{N-1}(t) = \eta_1(t), \tag{2.4e}$$
$$v'_{N-1}(t) = \eta_2(t), \tag{2.4f}$$

where $u_i(t) = u(x_i, t)$ and $v_i(t) = v(x_i, t)$ for $i = 0, \ldots, N-1$, the functions ζ_1, ζ_2, η_1 and η_2 are determined by the spatial discretization of boundary conditions and $\Delta_n[\phi_i(t), h]$ (with $\phi_i(t) = u_i(t)$ or $\phi_i(t) = v_i(t)$) is the n-point finite difference formula used to approximate the spatial second derivatives. The system (2.4) is also equipped by initial conditions

$$u_i(0) = \psi_1(x_i), \quad v_i(0) = \psi_2(x_i), \quad i = 0, \ldots, N - 1. \tag{2.5}$$

General purpose formulae for the numerical approximation of derivatives are constructed in order to be exact (within round-off error) on polynomials up to a certain degree. However, the resulting methods could require a very small stepsize in order

to follow the prescribed oscillations of the solution in case of problems generating periodic wavefronts. For this reason, as in [10, 11], we approximate the second spatial derivatives of functions u and v in (1.1) by the adapted three-point finite difference formula

$$\Delta_3[\phi_i(t), h] = \frac{1}{h^2} \left(a_0(z)\, \phi_{i+1}(t) + a_1(z)\, \phi_i(t) + a_2(z)\, \phi_{i-1}(t) \right), \tag{2.6}$$

where $z = \mu h$, whose coefficients are calculated in order to achieve the exactness (within round-off error) on functions belonging to the fitting space

$$\mathcal{F} = \{1, \sin(\mu x), \cos(\mu x)\}, \tag{2.7}$$

with spatial frequency $\mu \in \mathbb{R}$. We observe that this choice is motivated by the periodicity of the exact solution, a-priori known. Thus, as shown in [10], the expressions of the coefficients a_0, a_1 and a_2 are

$$a_0(z) = \frac{z^2}{2(1 - \cos z)} = a_2(z), \quad a_1(z) = -\frac{z^2}{1 - \cos z}. \tag{2.8}$$

Such coefficients are no longer constant, as in general purpose formulae, but depend on the parameter μ. In general, $z \neq 0$ because $h \neq 0$ and the frequency is not null in case of periodic solutions. Moreover, when z tends to 0, the variable coefficients (2.8) tend to the classic ones

$$a_0 = a_2 = 1, \quad a_1 = -2. \tag{2.9}$$

Therefore, the trigonometrically fitted formula preserves the second order of accuracy of the corresponding classic one, as shown in [10].

With regards to the time integration, we recast the system (2.4c)-(2.4d) in a more compact form:

$$\begin{aligned} U'(t) &= d_1\, A(z)U(t) + F_1(U(t), V(t)), \\ V'(t) &= d_2\, A(z)V(t) + F_2(U(t), V(t)), \end{aligned} \tag{2.10}$$

with

$$U(t) = \begin{bmatrix} u_1(t) \\ u_2(t) \\ \vdots \\ u_{N-2}(t) \end{bmatrix}, \quad F_1(t) = \begin{bmatrix} f_1(u_1(t), v_1(t)) \\ f_1(u_2(t), v_2(t)) \\ \vdots \\ f_1(u_{N-2}(t), v_{N-2}(t)) \end{bmatrix},$$

$$V(t) = \begin{bmatrix} v_1(t) \\ v_2(t) \\ \vdots \\ v_{N-2}(t) \end{bmatrix}, \quad F_2(t) = \begin{bmatrix} f_2(u_1(t), v_1(t)) \\ f_2(u_2(t), v_2(t)) \\ \vdots \\ f_2(u_{N-2}(t), v_{N-2}(t)) \end{bmatrix},$$

$$\gamma(z) = \frac{z^2}{2(1 - \cos z)}, \quad A(z) = \frac{\gamma(z)}{h^2} \begin{bmatrix} a_{1,1} & a_{1,2} & & & \\ 1 & -2 & 1 & & \\ & \ddots & \ddots & & \\ & & 1 & -2 & 1 \\ & & & a_{N-2,N-3} & a_{N-2,N-2} \end{bmatrix},$$

4

where the first and the last row of $A(z)$ are obtained by the spatial discretization of boundary conditions.

The terms in (2.10) exhibit a different nature: indeed, the one coming from the diffusion term is typically stiff, while that arising from the reaction component is assumed to be relatively nonstiff. As highlighted in Section 1, it may be convenient to use IMEX methods because they implicitly integrate only stiff components and explicitly integrate the others (see [1, 2, 3, 4, 31] and references therein), with a benefit in terms of efficiency in comparison with fully implicit methods, as well as on stability in comparison with explicit methods.

Thus, we consider a uniform time grid of M points

$$t_j = jk, \quad j = 0, 1, \ldots, M - 1,$$

in $[0, T]$, with the time step k, and we apply the linear first order IMEX-Euler method [2]

$$\phi^{j+1} = \phi^j + k\, G(\phi^{j+1}) + kF(\phi^j), \tag{2.11}$$

where G represents the diffusion term and F the reaction one. Hence, the numerical scheme for (2.10) is

$$\begin{aligned} U^{j+1} &= U^j + k\, d_1\, A^{j+1} U^{j+1} + k\, F_1(U^j, V^j), \\ V^{j+1} &= V^j + k\, d_2\, A^{j+1} V^{j+1} + k\, F_2(U^j, V^j), \end{aligned} \tag{2.12}$$

or, in a more compact form,

$$W^{j+1} = W^j + k\, \mathcal{A}^{j+1} W^{j+1} + k\, F(W^j), \tag{2.13}$$

where

$$W = \begin{bmatrix} U \\ V \end{bmatrix}, \quad \mathcal{A}^{j+1} = \begin{bmatrix} d_1 A^{j+1} & \\ & d_2 A^{j+1} \end{bmatrix}, \quad F = \begin{bmatrix} F_1 \\ F_2 \end{bmatrix}.$$

The matrix $\mathcal{A}$ depends on the parameter μ which has to be approximated. The selection strategy is object of the following sections.

3. Accuracy analysis

We now provide an accuracy analysis of the method (2.13), denoted as IMEX-EF in the remainder of the paper. In particular, Theorem 3.1 shows that the order of consistency of the numerical scheme is $O(z^2) + O(k)$. This result is coherent with the expectations since the fitted finite difference formula employed to approximate spatial derivatives has order 2 and depends on z and the IMEX-Euler method has order 1.

Theorem 3.1. *The IMEX-EF method* (2.13) *is consistent with the problem* (1.1) *and the order of consistency is* $O(z^2) + O(k)$*, where* $z = \mu h$ *as in* (2.8) *with spatial grid width h and k is the time stepsize.*

5

Proof: The local truncation error at the $(i, j + 1)$-grid point is

$$P_{h,k}^{i,j+1}[\phi] = \frac{\phi(x_i, t_{j+1}) - \phi(x_i, t_j)}{k} - f_\phi \left(u(x_i, t_j), v(x_i, t_j) \right)$$
$$- \frac{\gamma(z) \, d_\phi}{h^2} \left(\phi(x_{i+1}, t_{j+1}) - 2\phi(x_i, t_{j+1}) + \phi(x_{i-1}, t_{j+1}) \right), \tag{3.14}$$

where $\phi = u$ or $\phi = v$ and

$$d_\phi = d_1 \text{ and } f_\phi = f_1 \quad \text{if } \phi = u,$$
$$d_\phi = d_2 \text{ and } f_\phi = f_2 \quad \text{if } \phi = v.$$

We compute the following Taylor series expansions in order to appropriately rewrite the residual operator (3.14)

$$\phi(x_i, t_{j+1}) = \phi(x_i, t_j) + k \left(\frac{\partial \phi}{\partial t} \right)_{i,j} + \frac{k^2}{2} \left(\frac{\partial^2 \phi}{\partial t^2} \right)_{i,j} + O(k^3), \tag{3.15a}$$

$$\phi(x_{i+1}, t_{j+1}) = \phi(x_i, t_{j+1}) + h \left(\frac{\partial \phi}{\partial x} \right)_{i,j+1} + \frac{h^2}{2} \left(\frac{\partial^2 \phi}{\partial x^2} \right)_{i,j+1} + O(h^3), \tag{3.15b}$$

$$\phi(x_{i-1}, t_{j+1}) = \phi(x_i, t_{j+1}) - h \left(\frac{\partial \phi}{\partial x} \right)_{i,j+1} + \frac{h^2}{2} \left(\frac{\partial^2 \phi}{\partial x^2} \right)_{i,j+1} + O(h^3), \tag{3.15c}$$

$$\left(\frac{\partial^2 \phi}{\partial x^2} \right)_{i,j+1} = \left(\frac{\partial^2 \phi}{\partial x^2} \right)_{i,j} + k \left[\frac{\partial}{\partial t} \left(\frac{\partial^2 \phi}{\partial x^2} \right) \right]_{i,j} + \frac{k^2}{2} \left[\frac{\partial^2}{\partial t^2} \left(\frac{\partial^2 \phi}{\partial x^2} \right) \right]_{i,j} + O(k^3). \tag{3.15d}$$

We next reformulate the equation (3.15a) as follows

$$\frac{\phi(x_i, t_{j+1}) - \phi(x_i, t_j)}{k} = \left(\frac{\partial \phi}{\partial t} \right)_{i,j} + \frac{k}{2} \left(\frac{\partial^2 \phi}{\partial t^2} \right)_{i,j} + O(k^2), \tag{3.16}$$

and we sum (3.15b) and (3.15c), taking into account (3.15d):

$$\phi(x_{i+1}, t_{j+1}) - 2\phi(x_i, t_{j+1}) + \phi(x_{i-1}, t_{j+1}) =$$
$$h^2 \left(\frac{\partial^2 \phi}{\partial x^2} \right)_{i,j} + h^2 k \left[\frac{\partial}{\partial t} \left(\frac{\partial^2 \phi}{\partial x^2} \right) \right]_{i,j} + O(k^2 h^2) + O(h^4).$$

We now expand $\gamma(z)$ in power series, obtaining

$$\gamma(z) = 1 + \frac{z^2}{12} + \frac{z^4}{240} + O(z^6).$$

Hence, the local truncation error (3.14) becomes

$$
P_{h,k}^{i,j+1}[\phi] = \left(\frac{\partial \phi}{\partial t}\right)_{i,j} + \frac{k}{2}\left(\frac{\partial^2 \phi}{\partial t^2}\right)_{i,j} + O(k^2) - f_\phi(u(x_i, t_j), v(x_i, t_j))
$$

$$
- \frac{d_\phi}{h^2}\left[1 + \frac{z^2}{12} + O(z^4)\right]\left[h^2\left(\frac{\partial^2 \phi}{\partial x^2}\right)_{i,j} + h^2 k\left(\frac{\partial}{\partial t}\left(\frac{\partial^2 \phi}{\partial x^2}\right)\right)_{i,j} + O(h^2 k^2) + O(h^4)\right]
$$

$$
= \left(\frac{\partial \phi}{\partial t}\right)_{i,j} - f_\phi(u(x_i, t_j), v(x_i, t_j)) - d_\phi\left(\frac{\partial^2 u}{\partial x^2}\right)_{i,j} + O(k^2)
$$

$$
+ k\left[\frac{1}{2}\left(\frac{\partial^2 \phi}{\partial t^2}\right)_{i,j} - d_\phi\left(\frac{\partial}{\partial t}\left(\frac{\partial^2 \phi}{\partial x^2}\right)\right)_{i,j}\right] + O(h^2)
$$

$$
- d_\phi\left[\frac{z^2}{12} + O(z^4)\right]\left[\left(\frac{\partial^2 \phi}{\partial x^2}\right)_{i,j} + k\left(\frac{\partial}{\partial t}\left(\frac{\partial^2 \phi}{\partial x^2}\right)\right)_{i,j} + O(k^2) + O(h^2)\right].
$$

Since $\phi(x, t)$ is the exact solution of the problem (1.1), the following equation is verified

$$
\left(\frac{\partial \phi}{\partial t}\right)_{i,j} - d_\phi\left(\frac{\partial^2 \phi}{\partial x^2}\right)_{i,j} - f_\phi(u(x_i, t_j), v(x_i, t_j)) = 0,
$$

and the local truncation error assumes the expression

$$
P_{h,k}^{i,j+1}[\phi] = k\left[\frac{1}{2}\left(\frac{\partial^2 \phi}{\partial t^2}\right)_{i,j} - d_\phi\left(\frac{\partial}{\partial t}\left(\frac{\partial^2 \phi}{\partial x^2}\right)\right)_{i,j}\right] + O(k^2) + O(h^2)
$$

$$
- d_\phi\frac{z^2}{12}\left(\frac{\partial^2 \phi}{\partial x^2}\right)_{i,j} + O(z^4)
$$

$$
- d_\phi\left[\frac{z^2}{12} + O(z^4)\right]\left[k\left(\frac{\partial}{\partial t}\left(\frac{\partial^2 \phi}{\partial x^2}\right)\right)_{i,j} + O(k^2) + O(h^2)\right]
$$

$$
= O(k) + O(z^2).
$$

□

Theorem 3.1 is fundamental to prove the convergence of the numerical scheme (2.12), as shown in the following theorem:

Theorem 3.2. *Suppose that the vector valued function $F(W(\cdot, t_j))$ is smooth enough and satisfies the bound*

$$
\|\nabla F\|_2 \le F_{max}.
$$

Then, the global error

$$
E^{j+1} = W(\cdot, t_{j+1}) - W^{j+1}
$$

fulfills the bound

$$
\left\|E^{j+1}\right\|_2 \le \sum_{s=1}^{j+1}(1 + k\,F_{max})^{j+1-s}\left\|\mathcal{R}_{h,k}^{(s)}\right\|_2
$$

with $\mathcal{R}_{h,k}^{(j+1)} = O(k) + O(z^2)$. In other terms, under the above hypothesis, the IMEX-EF *method (2.13) is convergent.*

Proof: The discretization error in a fixed time grid point t_{j+1} is

$$E^{j+1} = W(\cdot, t_{j+1}) - W^{j+1}, \tag{3.17}$$

where $W(\cdot, t_{j+1})$ is the exact solution in t_{j+1}. Consistency of the method (see Theorem 3.1) implies that

$$W(\cdot, t_{j+1}) = W(\cdot, t_j) + k \, \mathcal{A} \, W(\cdot, t_{j+1}) + k \, F(W(\cdot, t_j)) + \mathcal{R}_{h,k}^{(j+1)}, \tag{3.18}$$

where $\mathcal{R}_{h,k}^{(j+1)} = O(k) + O(z^2)$.
Hence, the discretization error (3.17) becomes

$$
\begin{aligned}
E^{j+1} &= W(\cdot, t_j) + k \, \mathcal{A} \, W(\cdot, t_{j+1}) + k \, F(W(\cdot, t_j)) + \mathcal{R}_{h,k}^{(j+1)} - \\
&\quad - W^j - k \, \mathcal{A} \, W^{j+1} - k \, F(W^j) \\
&= E^j + k \, \mathcal{A} \, E^{j+1} + k \, [F(W(\cdot, t_j)) - F(W^j)] + \mathcal{R}_{h,k}^{(j+1)}.
\end{aligned}
\tag{3.19}
$$

Since $(I - k \, \mathcal{A})^{-1}$ is non-singular, the discretization error in t_{j+1} is

$$E^{j+1} = (I - k \, \mathcal{A})^{-1} \left(E^j + k \left(F(W(\cdot, t_j)) - F(W^j) \right) + \mathcal{R}_{h,k}^{(j+1)} \right), \tag{3.20}$$

which leads to the following relation

$$\left\| E^{j+1} \right\|_2 \leq \left\| (I - k \, \mathcal{A})^{-1} \right\|_2 \left(\left\| E^j \right\|_2 + k \left\| F(W(\cdot, t_j)) - F(W^j) \right\|_2 + \left\| \mathcal{R}_{h,k}^{(j+1)} \right\|_2 \right). \tag{3.21}$$

Since F is smooth enough for hypothesis, we can apply the mean value theorem:

$$\left\| F(W(\cdot, t_j)) - F(W^j) \right\|_2 = \|\nabla F\|_2 \left\| W(\cdot, t_j) - W^j \right\|_2 = \|\nabla F\|_2 \left\| E^j \right\|_\infty.$$

Moreover, the assumption $\|\nabla F\|_2 \leq F_{max}$ leads to

$$\left\| F(W(\cdot, t_j)) - F(W^j) \right\|_2 \leq F_{max} \left\| E^j \right\|_2. \tag{3.22}$$

In order to bound $\left\| (I - k \, \mathcal{A})^{-1} \right\|_2$, we observe that

$$(I - k \, \mathcal{A})^{-1} = Q^{\mathsf{T}} (I - k \, \mathcal{A}_\lambda)^{-1} Q,$$

where Q is an orthogonal matrix and $\mathcal{A}_\lambda$ is a diagonal matrix having the eigenvalues of $\mathcal{A}$ on the diagonal. We next recall that $\|Q\|_2 = 1 = \|Q^{\mathsf{T}}\|_2$ and the eigenvalues of $\mathcal{A}$

$$\lambda_k = -d_\phi \, \frac{4\gamma(z)}{h^2} \, \sin^2 \left(\frac{k\pi}{2(N-1)} \right) \leq 0, \quad k = 1, 2, \ldots, N-2,$$

so the following bound holds

$$\left\| (I - k \, \mathcal{A}_\lambda)^{-1} \right\|_2 = \rho((I - k \, \mathcal{A})^{-1}) = \frac{1}{1 - k \, \lambda_{max}} \leq 1, \tag{3.23}$$

8

where λ_{max} is the eigenvalue of $\mathcal{A}$ with the highest modulus. Therefore, the norm of the discretization error is given by

$$\begin{aligned}
\left\|E^{j+1}\right\|_2 &\leq \left\|E^j\right\|_2 + k\left\|F(W(\cdot,t_j)) - F(W^j)\right\|_2 + \left\|\mathcal{R}_{h,k}^{(j+1)}\right\|_2 \\
&\leq (1 + k\,F_{max})\left\|E^j\right\|_2 + \left\|\mathcal{R}_{h,k}^{(j+1)}\right\|_2.
\end{aligned} \tag{3.24}$$

We recursively apply this relation until the discretization error at first step appears, as follows:

$$\left\|E^{j+1}\right\|_2 \leq (1 + k\,F_{max})^2\left\|E^{j-1}\right\|_2 + (1 + k\,F_{max})\left\|\mathcal{R}_{h,k}^{(j)}\right\|_2 + \left\|\mathcal{R}_{h,k}^{(j+1)}\right\|_2$$

$$\ldots \leq (1 + k\,F_{max})^{j+1}\left\|E^0\right\|_2 + \sum_{s=1}^{j+1}(1 + k\,F_{max})^{j+1-s}\left\|\mathcal{R}_{h,k}^{(s)}\right\|_2$$

Since $\left\|E^0\right\|_2 = 0$, we obtain for each j

$$\left\|E^{j+1}\right\|_2 \leq \sum_{s=1}^{j+1}(1 + k\,F_{max})^{j+1-s}\left\|\mathcal{R}_{h,k}^{(s)}\right\|_2 \xrightarrow[h,k\to 0]{} 0.$$

$\square$

4. Parameter selection

This section is devoted to introducing a selection strategy for the estimation of the parameter μ in (2.7), necessary for the computation of the coefficients (2.8). This is a crucial problem in applying exponentially fitted methods (see [18, 20] and references therein), because their coefficients are no longer constant as it happens for traditional methods based on algebraic polynomials, but depend on the values of unknown parameters. The problem of estimating the parameters has been handled, up to now, by minimizing or annihilating the principal term of the local truncation error associated to the method (see [8, 9, 16, 18, 20] and references therein). We aim to follow a similar path, i.e. we estimate the value of μ by minimizing the leading term of the local truncation error, whose expression in each grid point is provided in the proof of the Theorem 3.1, as follows:

$$\begin{aligned}
P_{h,k}^{i,j+1}[\phi] = &k\left[\frac{1}{2}\left(\frac{\partial^2 \phi}{\partial t^2}\right)_{i,j} - \left(\frac{\partial}{\partial t}\left(\frac{\partial^2 \phi}{\partial x^2}\right)\right)_{i,j}\right] + O(k^2) + O(h^2) \\
&- d_\phi \frac{z^2}{12}\left(\frac{\partial^2 \phi}{\partial x^2}\right)_{i,j} + O(z^2 k) + O(z^4),
\end{aligned} \tag{4.25}$$

where $\phi = u$ or $\phi = v$, $d_\phi = d_1$ if $\phi = u$ and $d_\phi = d_2$ if $\phi = v$ and $z = \mu h$. Its μ-dependent leading term is

$$T^{i,j+1}(\mu) = -d_\phi \frac{\mu^2 h^2}{12}\left(\frac{\partial^2 \phi}{\partial x^2}\right)_{i,j}. \tag{4.26}$$

9

We recall that the exact solution ϕ relies on the parameter μ because in a problem-oriented approach it is assumed to belong to the space spanned by the basis functions (2.7). Since we want to minimize (4.26), we approximate the spatial second derivative by the fitted finite difference formula (2.6) with coefficients (2.8):

$$\overline{T}^{i,j+1}(\mu) = d_\phi \frac{\mu^2 z^2 \left(2\phi_i^j - \phi_{i+1}^j - \phi_{i-1}^j\right)}{24(1 - \cos z)}. \tag{4.27}$$

Therefore, we can calculate the optimal parameter in each inner grid point by minimizing the function (4.27). In order to perform such a minimization we compute the first derivative of (4.27) with respect to μ

$$\frac{d\overline{T}^{i,j+1}}{d\mu}(\mu) = d_\phi \frac{z^2 \left(2\phi_i^j - \phi_{i+1}^j - \phi_{i-1}^j\right)}{24} \frac{\mu \left(4(1 - \cos z) - z \sin z\right)}{(1 - \cos z)^2}, \tag{4.28}$$

and annihilate it. Since

$$\frac{d_\phi \, z^2}{24 \, (1 - \cos z)^2} > 0,$$

and $\mu \neq 0$, we solve the nonlinear equation

$$(4(1 - \cos z) - z \sin z) \left(2\phi_i^j - \phi_{i+1}^j - \phi_{i-1}^j\right) = 0.$$

As also shown in Figure 1, the function

$$D(z) = 4(1 - \cos z) - z \sin z$$

has roots in $z = 0, \pm 2\pi, \pm 8.55, \ldots$. Therefore, we can select

$$\overline{\mu}_{i,j+1} = \pm \frac{8.55}{h}$$

as points of relative minimum for $\overline{T}^{i,j+1}$.
In order to improve this estimate by adding a correction term, we assume that

$$\frac{\alpha_{i,j}^2}{h^2} \leq 1, \tag{4.29}$$

where $\alpha_{i,j} = 2\phi_i^j - \phi_{i+1}^j - \phi_{i-1}^j$, such that the following relation holds

$$\left|T^{i,j+1}(\overline{\mu}_{i,j+1})\right| = \left|-\left(\frac{\partial^2 \phi}{\partial x^2}\right)_{i,j}\right| d_\phi \frac{\beta^2}{12} \geq \left|-\left(\frac{\partial^2 \phi}{\partial x^2}\right)_{i,j}\right| d_\phi \frac{\beta^2}{12} \frac{\alpha_{i,j}^2}{h^2}, \tag{4.30}$$

where $\beta = 8.55$. Therefore, the leading term (4.26) of the local truncation error is smaller in modulus when it is evaluated in $\mu_{i,j+1} = \frac{\beta}{h^2}\alpha_{i,j}$. Hence, we propose an estimation of the optimal parameter relying on the additional grid-dependent correction term $\frac{\alpha_{i,j}}{h}$, i.e.

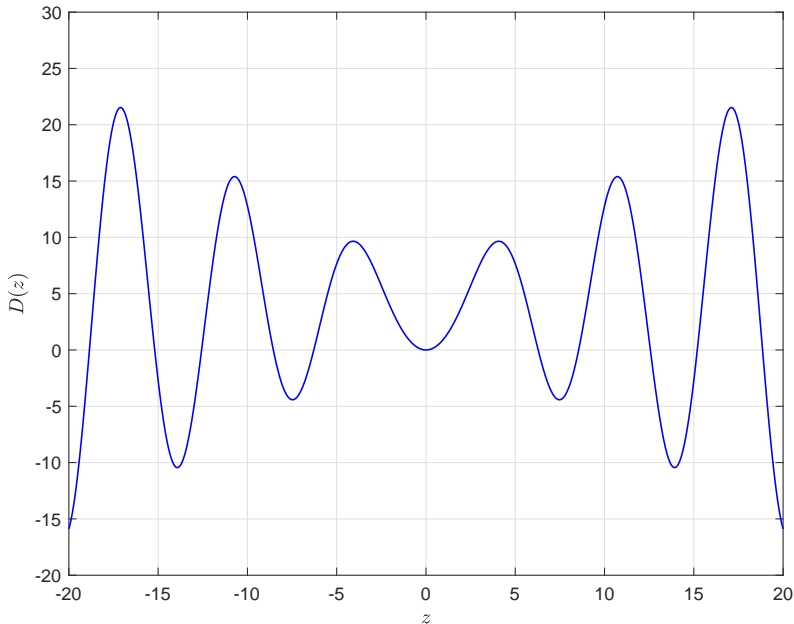$$\mu_{i,j+1}^{OPT} = \frac{8.55}{h^2}\alpha_{i,j}. \tag{4.31}$$

10

Figure 1: Plot of $D(z) = 4(1 - \cos z) - z \sin z$, where $z = \mu h$, μ is the parameter which the basis functions (2.7) depend on and h is the spatial stepsize. The study of this function is necessary for the parameter selection presented in Section 4.

It is important to highlight that the proposed estimation (4.31) only depends on values already computed and does not require the further solution of nonlinear equations or minimization problems in applying the numerical scheme, as it happens, for instance, in [8, 9, 16]. Moreover, we remark that condition (4.29) does not impose any further strict restrictions on the stepsize. Therefore, the presented parameter selection does not increase a lot the computational cost. Moreover, the proposed estimate is adapted to the numerical scheme because it is obtained by minimizing the corresponding local truncation error. Finally, although the frequency of the oscillations in the exact solution is constant, the parameter is computed at each grid point, so the estimate is accurately tuned to the problem (as also shown in Figure 2 and Figure 6), and an extreme accumulation of the global error is avoided.

5. Numerical experiments

We now show the numerical evidence arising from the integration of some test reaction-diffusion systems by means of the IMEX-EF method (2.13). In each considered test, we prove that the term coming from the diffusion exhibits an higher stiffness

11

than the component arising from the reaction, so an IMEX integration is worthwhile. For this purpose, we compute the stiffness ratio of the matrix $\mathcal{A}$ arising from the discretization of the diffusion term, as follows:

$$\mathcal{R}_{df} = \frac{|\text{Re}(\bar{\lambda})|}{|\text{Re}(\underline{\lambda})|} = \frac{\sin^2\left(\dfrac{\pi(N-2)}{2(N-1)}\right)}{\sin^2\left(\dfrac{\pi}{2(N-1)}\right)}, \tag{5.32}$$

where $\bar{\lambda}$ and $\underline{\lambda}$ are the eigenvalues of the matrix $\mathcal{A}$ such that

$$|\text{Re}(\bar{\lambda})| \geq |\text{Re}(\lambda_i)| \geq |\text{Re}(\underline{\lambda})|, \quad i = 1, \dots, N-2.$$

On the other hand, we calculate the stiffness ratio $\mathcal{R}_{rt}$ of the Jacobian matrix related to the reaction term in order to study the stiffness of this component.

In the remainder of this section, we refer to the method (2.13) presented in this paper as IMEX-EF. On the other side, we call IMEX-classic the scheme obtained by discretizing in space the system of PDEs through the method of lines and the traditional three-point finite difference formula and then integrating in time the resulting system of ODEs by means of the IMEX Euler method (2.11). We remark that the classic three-point finite difference formula is constructed in order to be exact (within round-off error) on polynomials up to a certain degree and its coefficients are reported in Equation (2.9).

5.1. Linear test problem

We consider the following test reaction-diffusion problem

$$\begin{aligned}
\frac{\partial u}{\partial t} &= \frac{\partial^2 u}{\partial x^2} + u, \\
\frac{\partial v}{\partial t} &= \frac{\partial^2 v}{\partial x^2} + v + 1,
\end{aligned} \tag{5.33}$$

with $u, v : [0, 4\pi] \times [0, 1] \longrightarrow \mathbb{R}$, with initial conditions

$$u(x, 0) = \sin x, \quad v(x, 0) = \cos x - 1, \tag{5.34}$$

and homogeneous Dirichlet boundary conditions

$$u(0, t) = 0, \quad v(0, t) = 0, \quad u(4\pi, t) = 0, \quad v(4\pi, t) = 0. \tag{5.35}$$

The exact solution

$$u(x, t) = \sin x, \quad v(x, t) = \cos x - 1 \tag{5.36}$$

oscillates in space with a spatial frequency equal to 1, so the use of the trigonometrical fitting space (2.7) is justified and the exact value for the parameter μ is equal to the spatial frequency, i.e. $\mu_{exact} = 1$. Moreover, the stiffness ratio of the Jacobian matrix related to the reaction term is equal to 1, whereas the stiffness ratio (5.32) of the matrix $\mathcal{A}$ arising from the discretization of the diffusion term increases with the number of

12

Method	h	$\mathcal{R}_{\mathbf{df}}$	Timing [s]	Error
IMEX-EF	$\pi/5$	161.4	10.8	$4.9 \cdot 10^{-16}$
IMEX-classic	$\pi/5$	161.4	5.4	$3.3 \cdot 10^{-2}$
IMEX-classic	$\pi/10$	647.8	8.5	$8.2 \cdot 10^{-3}$
IMEX-classic	$\pi/20$	$2.6 \cdot 10^3$	17.3	$2.0 \cdot 10^{-3}$
IMEX-classic	$\pi/40$	$1.0 \cdot 10^4$	37.8	$5.1 \cdot 10^{-4}$

Table 1: Comparison between the IMEX-EF (2.13) joined with the exact value for the parameter $\mu_{exact} = 1$ and the corresponding classic IMEX in terms of spent time and error for the numerical integration of system (5.33) provided with the initial conditions (5.34) and boundary conditions (5.35). The error has been computed as difference with respect to the exact solution (5.36). In all the presented tests, the time stepsize is $k = 0.01$ and $\mathcal{R}_{df}$ is the stiffness ratio (5.32) of the matrix $\mathcal{A}$ arising from the discretization of the Laplacian operator.

grid points N, as it is shown in Table 1. Therefore, the diffusion term is much more stiff than the reaction one and the adoption of an IMEX integration is justified.

Table 1 also shows that the IMEX-EF scheme is extremely more accurate than the IMEX-classic. Moreover, the classic scheme does not achieve the same accuracy of IMEX-EF when it takes the same time (see Table 1 for $h = \pi/10$ and $h = \pi/20$). For this reason, when the exact value for the parameter is available, it appears clear that IMEX-EF is much more convenient. However, the error drastically increases if the value of parameter μ is far from the exact value $\mu_{exact} = 1$, as it is exhibited in Table 2. In particular, we observe that for $\mu = 0.2$ IMEX-EF achieves a similar accuracy with respect to the classic one, but dramatically increasing the computational cost. Therefore, the advantages of an adapted scheme are strongly influenced by the value of the parameter μ, so a proper strategy is required to estimate this parameter, when it is unknown. Table 2 shows that IMEX-EF combined with the estimate (4.31) proposed in Section 4 is as accurate as the same scheme joined with the exact value, but it is obviously more expensive because it requires the computation of the parameter at each grid point. Finally, in Figure 2 we observe that the estimated paramater is generally close to the exact value ($\mu = 1$) and the fact that the estimate is point-wise avoids the increase of the error in those cases when the parameters is far from 1.

5.2. λ-ω problems

Among reaction-diffusion problems, the so-called λ-ω systems represent one of the most studied classes [14, 15, 19, 24, 25], especially for their important property of generating periodic plane waves. In general, they have the following expression:

$$
\begin{aligned}
\frac{\partial u}{\partial t} &= d_1 \frac{\partial^2 u}{\partial x^2} + \lambda(r)u - \omega(r)v, \\
\frac{\partial v}{\partial t} &= d_2 \frac{\partial^2 v}{\partial x^2} + \omega(r)u + \lambda(r)v,
\end{aligned}
\tag{5.37}
$$

Method	μ	Timing [s]	Error
IMEX-EF	1	40.7	$4.9 \cdot 10^{-16}$
IMEX-EF	0.8	92.9	$7.3 \cdot 10^{-4}$
IMEX-EF	0.2	92.6	$2.0 \cdot 10^{-3}$
IMEX-classic	–	17.3	$2.0 \cdot 10^{-3}$
IMEX-EF	opt	71.9	$4.9 \cdot 10^{-16}$

Table 2: Accuracy and efficiency of the IMEX-EF scheme (2.13) according to the value for the parameter μ within the numerical integration of the system (5.33) equipped with initial conditions (5.34) and boundary conditions (5.35). These results have been compared with that ones obtained with the classic IMEX scheme, the IMEX-EF scheme applied with the exact value for the parameter ($\mu_{exact} = 1$) and the IMEX-EF scheme joined with the estimated value for the parameter μ (4.31). In this test, the time stepsize is $k = 0.01$ and the spatial mesh width is $h = \pi/20$.

with $u, v : [0, \infty) \times [0, T] \longrightarrow \mathbb{R}$, $r = \sqrt{u^2 + v^2}$, $\omega(0) > 0$, $\lambda(0) > 0$. The nonlinearity visible in the reaction term is governed by the functions $\lambda(r)$ and $\omega(r)$ which are usually chosen as in [24]:

$$\lambda(r) = \lambda_0 - r^p, \quad \omega(r) = \omega_0 - r^p, \quad p > 0, \quad \lambda_0 > 0, \quad \omega_0 > 0. \tag{5.38}$$

We solve the system (5.37) equipped by the following initial data decaying exponentially in space on the semi-infinite domain $[0, \infty)$

$$u(x, 0) = v(x, 0) = \xi_1 \exp(-\xi_2 x), \tag{5.39}$$

and mixed boundary conditions

$$\frac{\partial u}{\partial x}(0, t) = \frac{\partial v}{\partial x}(0, t) = 0, \quad \lim_{x \to +\infty} u(x, t) = \lim_{x \to +\infty} v(x, t) = 0. \tag{5.40}$$

As proved in [19], the exact solution of (1.1) can be parametrized as

$$u(x, t) = \hat{r} \cos(\omega(\hat{r})t \pm \sqrt{\lambda(\hat{r})}x), \quad v(x, t) = \hat{r} \sin(\omega(\hat{r})t \pm \sqrt{\lambda(\hat{r})}x), \tag{5.41}$$

with $\hat{r} \in \mathbb{R}$ such that $\lambda(\hat{r}) > 0$. It depends on the parameter $\hat{r}$, so it is actually not computable. However, it is important to realize that it is a periodic plane wave, so it has constant shape and speed and oscillates both in space and in time, so it can be convenient to employ trigonometrically fitted formulae. Moreover, the stiffness ratio (5.32) of the matrix $\mathcal{A}$ coming from the discretization of the Laplacian operator is much higher than the stiffness ratio of the Jacobian matrix related to the reaction term: for instance, if $h = 1$ and $k = 0.5$, the stiffness ratio of the diffusive term is equal to 9118.2, while that of the reactive part is equal to 12.9. These features make the problem a good candidate for the adoption of the IMEX-EF (2.13) adapted method.

Following the ideas exposed in Section 2, we solve the problem in the domain $[0, X] \times [0, T]$ where X is large enough so that its further increases have negligible effects on
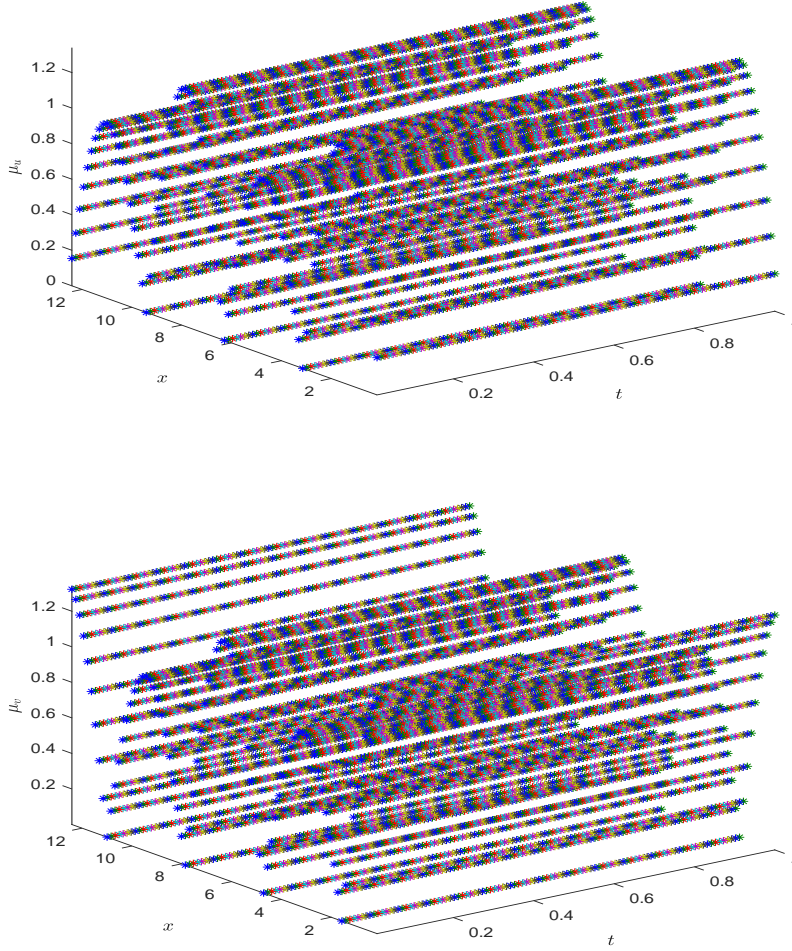
Figure 2: Estimated parameter μ for both components u (on the top) and v (on the bottom) of the solution in each grid point computed by the formula (4.31) according the optimization strategy described in Section 4, within the numerical integration of the system (5.33) equipped with initial conditions (5.34) and boundary conditions (5.35), and with $h = \pi/20$ and $k = 0.01$.

the solution. Thus, we reformulate the boundary conditions as follows

$$\frac{\partial u}{\partial x}(0, t) = \frac{\partial v}{\partial x}(0, t) = 0, \tag{5.42a}$$

$$u(X, t) = v(X, t) = 0. \tag{5.42b}$$

15

We apply the method (2.13) with

$$A(z) = \frac{\gamma(z)}{h^2} \begin{bmatrix} -2 & 2 & & & \\ 1 & -2 & 1 & & \\ & & \ddots & \ddots & \\ & & & 1 & -2 \end{bmatrix}, \quad F = \begin{bmatrix} \Lambda U - \Omega V \\ \Omega U + \Lambda V \end{bmatrix},$$

$$\Lambda(r) = \begin{bmatrix} \lambda(r) & & & \\ & \lambda(r) & & \\ & & \ddots & \\ & & & \lambda(r) \end{bmatrix}, \quad \Omega(r) = \begin{bmatrix} \omega(r) & & & \\ & \omega(r) & & \\ & & \ddots & \\ & & & \omega(r) \end{bmatrix},$$

and the following values for the parameters

$$d_1 = 1 = d_2, \quad \lambda_0 = 1, \quad \omega_0 = 2, \quad p = 1.8, \quad \xi_1 = 0.1, \quad \xi_2 = 0.8. \tag{5.43}$$

The rectangular domain is $\overline{\mathcal{D}} = [0,\, 150] \times [0,\, 60]$. It is useful to note that the spatial interval is large enough to justify the use of boundary conditions (5.42) instead of (5.40). For the application of method (2.13), we employ the parameter selection strategy discussed in Section 4, and compare this value with an additional estimate that can be desumed by the parametrization of the exact solution (5.41), i.e.

$$\mu_{ij}^{OPT} = \sqrt{\left|\lambda(r_{ij})\right|}, \tag{5.44}$$

where

$$r_{ij} = \sqrt{u_{ij}^2 + v_{ij}^2}, \tag{5.45}$$

with $u_{ij} \approx u(x_i, t_j)$, $v_{ij} \approx v(x_i, t_j)$. Parameter estimation is performed in each grid point, without heightening the computational cost of the solver at all. The reason why the estimation is not performed just once, even if the solution has constant frequency, is given by the fact that the numerical solution has not constant frequency, due to the accumulation of error, thus it is reasonable to recompute the approximated parameter point by point.

We observe that, for the numerical solution, the following relation holds

$$\frac{\alpha_{i,j}^2}{h^2} \leq 1,$$

which makes applicable the estimation strategy presented in Section 4.

For simplicity, we denote by IMEX-EF-PS the method IMEX-EF (2.13) combined to the problem-suggested estimate (5.44) and IMEX-EF-Opt the IMEX-EF method (2.13) joined with the estimate (4.31) computed as described in Section 4.

Figure 3 and Figure 4 exhibit the profiles of the solutions computed by the aforementioned methods (IMEX-EF-Opt and IMEX-EF-PS, respectively): we observe that they generate wavefronts moving along the domain with constant speed and shape. This behaviour is coherent with the expectations coming from previous studies (see

16

[24]) and the comparison with the solution obtained by the Matlab routine `pdepe` (see Figure 5). We recall that the Matlab routine `pdepe` is an automatic solver for the following class of PDEs:

$$c\left(x, t, \phi, \frac{\partial \phi}{\partial x}\right) \frac{\partial \phi}{\partial t} = x^{-m} \frac{\partial}{\partial x}\left(x^m f\left(x, t, \phi, \frac{\partial \phi}{\partial x}\right)\right) + s\left(x, t, \phi, \frac{\partial \phi}{\partial x}\right),$$

provided with proper initial and boundary conditions. We remark that problem (5.37) belongs to this class, by assuming

$$c\left(x, t, \phi, \frac{\partial \phi}{\partial x}\right) = [1, 1]^T, \quad f\left(x, t, \phi, \frac{\partial \phi}{\partial x}\right) = \left[\frac{\partial u}{\partial x}, \frac{\partial v}{\partial x}\right]^T,$$

$$s\left(x, t, \phi, \frac{\partial \phi}{\partial x}\right) = [\lambda(r)\, u - \omega(r)\, v, \; \omega(r)\, u + \lambda(r)\, v]^T, \quad m = 0.$$

The integration in space is carried out by employing finite differences depending on a number of points automatically chosen on a mesh provided by the user. The resulting system of ODEs is then solved through the Matlab routine `ode15s` which selects both timestep and solver automatically.

Figure 6 shows that the optimal estimate (4.31) follows the character of the problem much better than the problem-suggested estimate (5.44), even if both give a reasonable numerical solution. It is important to highlight that the estimate (5.44) requires the knowledge of at least a parametrization of the exact solution, which is not always possible to be computed, while the estimate (4.31) does not need further a-priori known information on the solution of the problem. Therefore, the numerical scheme IMEX-EF-Opt can be thought as preferable with respect to the scheme IMEX-EF-PS.

Finally, Figure 7 and Figure 8 highlight that the IMEX-EF method is much more stable than the corresponding classic one.

6. Conclusions

The work has focused on the numerical solution of reaction-diffusion system generating periodic wavefronts by means of a numerical scheme which relies on trigonometrically fitted finite differences for the space discretization and on an IMEX scheme for the discretization in time. The adoption of trigonometrically fitted formulae is
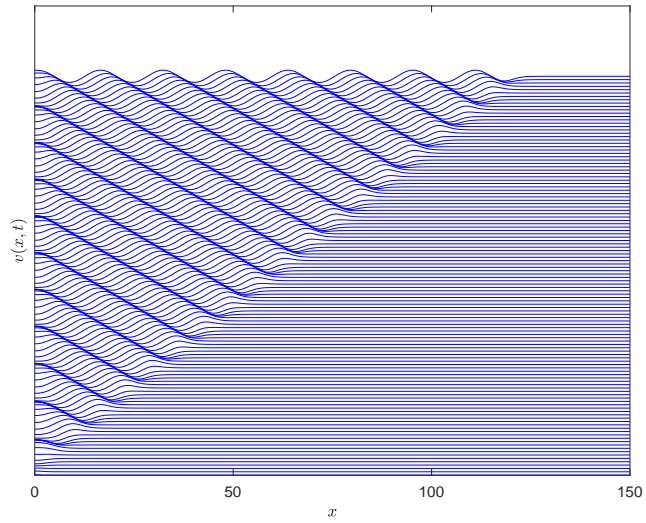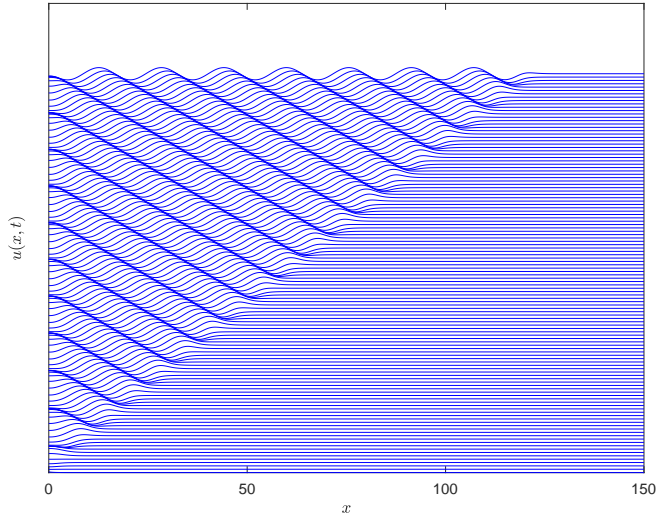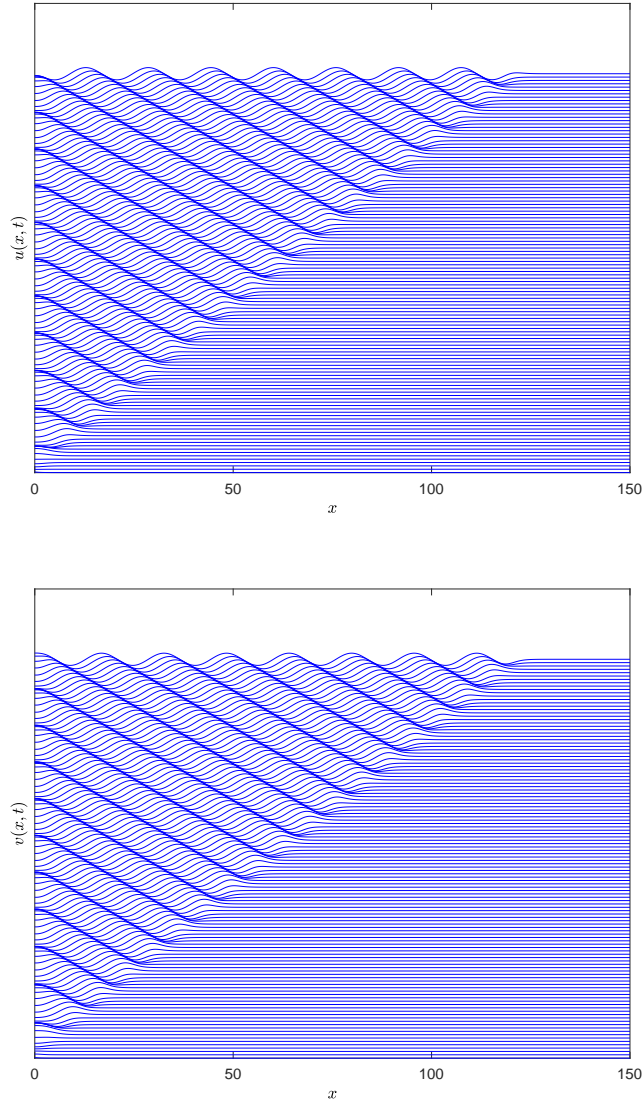
Figure 3: Numerical solutions of $\lambda - \omega$ reaction-diffusion system (5.37), with functions $\lambda(r)$ and $\omega(r)$ chosen as in (5.38), initial conditions (5.39) and boundary conditions (5.42), computed by the new method (2.13) with spatial stepsize $h = 0.3$ and time stepsize $k = 0.01$ and the estimate (4.31) for the parameter μ presented in Section 4. The solutions u (on the top) and v (on the bottom) are depicted as functions of space x at successive times t, with a vertical separation proportional to the time interval.

suggested by the a-priori known oscillatory behaviour of the exact solution and may guarantee a better balance between accuracy and efficiency with respect to classic
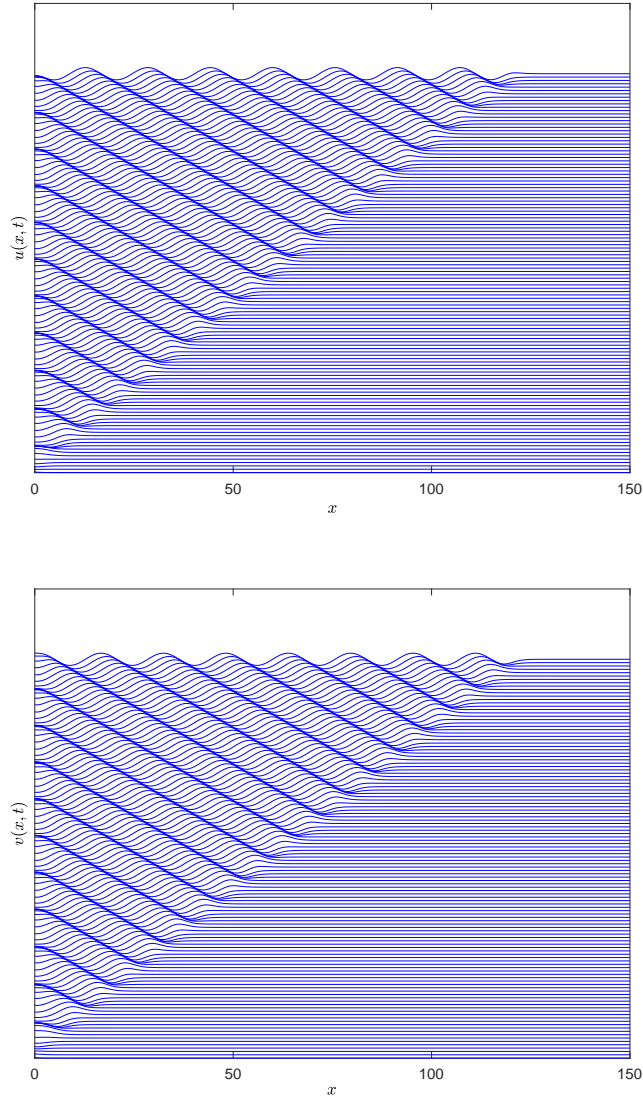
18

Figure 4: Numerical solutions of $\lambda - \omega$ reaction-diffusion system (5.37), with functions $\lambda(r)$ and $\omega(r)$ chosen as in (5.38), initial conditions (5.39) and boundary conditions (5.42), computed by the new method (2.13) with spatial stepsize $h = 0.3$ and time stepsize $k = 0.01$ and the problem-suggested estimate (5.44) for the parameter μ. The solutions u (on the top) and v (on the bottom) are depicted as functions of space x at successive times t, with a vertical separation proportional to the time interval.

methods. The used trigonometrically fitted finite differences depend on the values of unknown parameters related to the solution that have to be accurately estimated.

19

Figure 5: Numerical solution of $\lambda - \omega$ reaction-diffusion system (5.37), with functions $\lambda(r)$ and $\omega(r)$ chosen as in (5.38), initial conditions (5.39) and boundary conditions (5.42) computed by the Matlab routine pdepe with spatial stepsize $h = 0.3$ and a tolerance equal to 10^{-14}. The solutions u (on the top) and v (on the bottom) are depicted as functions of space x at successive times t, with a vertical separation proportional to the time interval.

The proposed estimation strategy, presented in Section 4, is particularly tuned to the numerical scheme, because it is based on minimizing the principal term of the corresponding local truncation error. It is worth highlighting that such an estimation of the
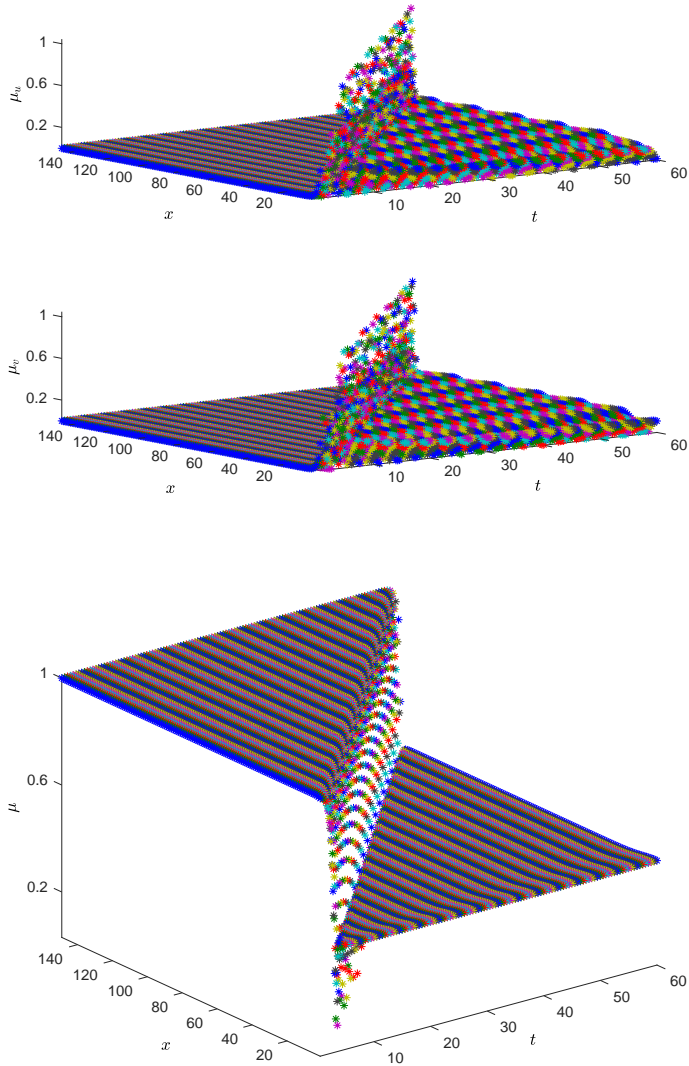
Figure 6: Estimated parameter in each grid point computed for the numerical integration of the system (5.37) with functions $\lambda(r)$ and $\omega(r)$ chosen as in (5.38), equipped by initial conditions (5.39) and boundary conditions (5.42) and with $h = 1$ and $k = 0.5$. Top figure: estimated parameter computed by the formula (4.31) described in Section 4. The parameter related to the component u is depicted on the top, whereas the parameter related to the component v is represented on the bottom. Bottom figure: estimated parameter (the same for both components) computed by employing the problem-suggested formula (5.44).

parameter does not require the employ of a minimization procedure or the solution of nonlinear systems of equations at each step, as in [8, 9, 16], but totally relies on the
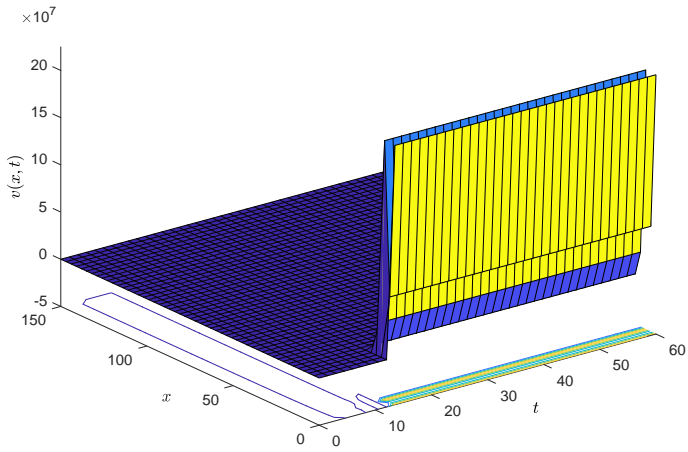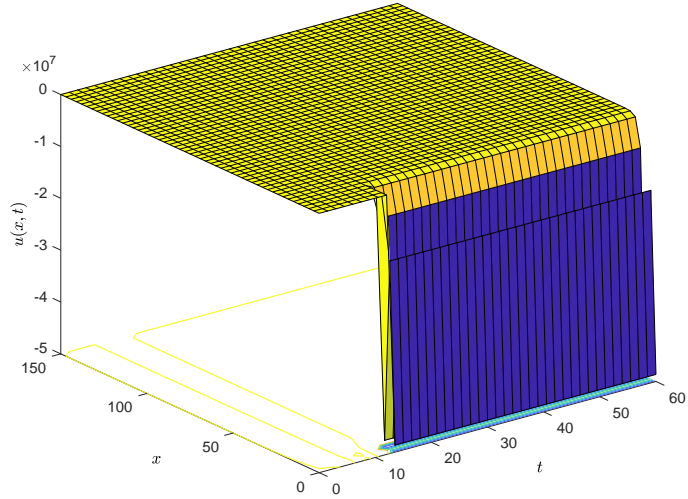
21

Figure 7: Numerical solutions of $\lambda - \omega$ reaction-diffusion system (5.37), with functions $\lambda(r)$ and $\omega(r)$ chosen as in (5.38), initial conditions (5.39) and boundary conditions (5.42) computed by IMEX-classic method with spatial grid width $h = 3$ and time stepsize $k = 1.5$. The component u is depicted on the top and the component v is represented on the bottom.

application of Equation (4.31), hence without a significant increment in the computational cost. Moreover, although the frequency of the oscillations in the exact solution is constant, the parameter is computed at each grid point, such that the estimate is
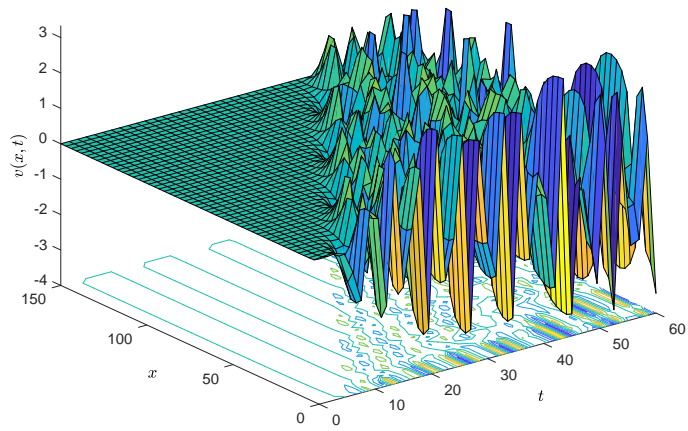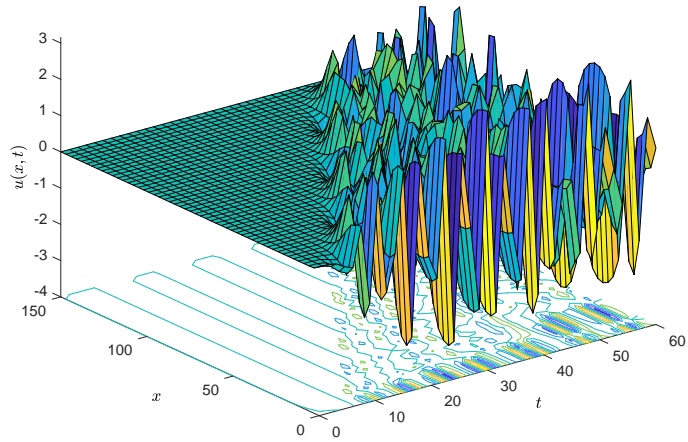
Figure 8: Numerical solutions of $\lambda - \omega$ reaction-diffusion system (5.37), with functions $\lambda(r)$ and $\omega(r)$ chosen as in (5.38), initial conditions (5.39) and boundary conditions (5.42) computed by IMEX-EF method with spatial grid width $h = 3$ and time stepsize $k = 1.5$. The component u is depicted on the top and the component v is represented on the bottom.

particularly adapted to the problem and a strong accumulation of the global error is avoided. Numerical experiments have shown the effectiveness of this approach, also in comparison with traditional finite difference schemes. In particular, we mean that

23

adapted schemes follow better the qualitative behaviour of the solutions. Finally, we remark that the choice of a proper fitting space is crucial to exploit all the benefits of exponential fitting strategy. Therefore, further contributions in this field will address the open problem of creating a better match between the choice of the basis and the estimate of the unknown parameters.

[1] Ascher, U.M., Ruuth, S.J., Spiteri, R.J.: Implicit-Explicit Runge-Kutta Methods for Time-Dependent Partial Differential Equations. Appl. Numer. Math. 25(2-3), 151–167 (1997).

[2] Ascher, U.M., Ruuth, S.J., Wetton, B.T.R.: Implicit-Explicit methods for time-dependent partial differential equations. SIAM J. Numer. Anal. 32, 797–823 (1995).

[3] Boscarino, S.: Error analysis of IMEX Runge-Kutta methods derived from differential-algebraic systems. SIAM J. Numer. Anal. 45(4), 1600–1621 (2007).

[4] Boscarino, S.: On an accurate third order implicit-explicit Runge-Kutta method for stiff problems. Appl. Numer. Math. 59(7), 1515–1528 (2009).

[5] Burrage, K., Cardone, A., D'Ambrosio, R., Paternoster, B.: Numerical solution of time fractional diffusion systems. Appl. Numer. Math. 116, 82–94 (2017).

[6] Cardone, A., D'Ambrosio, R., Paternoster, B.: Exponentially fitted IMEX methods for advection-diffusion problems. J. Comput. Appl. Math. 316, 100–108 (2017).

[7] D'Ambrosio, R., Moccaldi, M., Paternoster, B.: Adapted numerical methods for advection-reaction-diffusion problems generating periodic wavefronts. Comput. Math. Appl. 74(5), 1029–1042 (2017).

[8] D'Ambrosio, R., Esposito, E., Paternoster, P.: Exponentially fitted two-step Runge-Kutta methods: Construction and parameter selection. Appl. Math. Comp. 218 (14), 7468–7480 (2012).

[9] D'Ambrosio, R., Esposito, E., Paternoster, B.: Parameter estimation in exponentially fitted hybrid methods for second order ordinary differential problems. J. Math. Chem. 50, 155-168 (2012).

[10] D'Ambrosio, R., Paternoster, B.: Numerical solution of a diffusion problem by exponentially fitted finite difference methods. SpringerPlus 3:425 (2014).

[11] D'Ambrosio, R., Paternoster, B.: Numerical solution of reaction-diffusion systems of λ-ω type by trigonometrically fitted methods. J. Comput. Appl. Math. 294,436-445 (2016).

[12] D'Ambrosio, R., Paternoster, B., Santomauro, G.: Revised exponentially fitted Runge-Kutta-Nyström, methods. Appl. Math. Lett. 30, 56-60 (2014).

[13] Ferrell, J.E., Tsai, T.Y., Yang, Q.: Modeling the cell cycle: why do certain circuits oscillate?. Cell. 144(6), 874885 (2011).

[14] Garvie, M.R., Blowey, J.F.: A reaction-diffusion system of λ-ω type. Part II: Numerical analysis. Euro. J. Appl. Math. 16, 621–646 (2005).

[15] Greenberg, J.M.: Spiral waves for λ-ω systems. Adv. Appl. Math. 2, 450–455 (1981).

[16] Hollevoet, D., Van Daele, M., Vanden Berghe, G.: Exponentially-fitted methods applied to fourth order boundary value problems. J. Comput. Appl. Math. 235(18), 5380–5393 (2011).

[17] Isaacson, E., Keller, H.B.: Analysis of Numerical Methods. Dover Publications, New York (1994).

[18] Ixaru, L.Gr., Vanden Berghe, G.: Exponential Fitting. Kluwer, Boston-Dordrecht-London (2004).

[19] Kopell, N., Howard, L.N.: Plane waves solutions to reaction-diffusion equations. Stud. Appl. Math. 52, 291–328 (1973).

[20] Paternoster, B.: Present state-of-the-art in exponential fitting. A contribution dedicated to Liviu Ixaru on his 70-th anniversary. Comput. Phys. Commun. 183, 2499–2512 (2012).

[21] Ruuth, S.J.: Implicit-explicit methods for reaction-diffusion problems in pattern formation. J. Math. Biol. 34, 148–176 (1995).

[22] Schiesser, W.E.: The Numerical Method of Lines: Integration of Partial Differential Equations. Academic Press, San Diego (1991).

[23] Schiesser, W.E., Griffiths, G.W.: A Compendium of Partial Differential Equation Models: Method of Lines Analysis with Matlab. Cambridge University Press (2009).

[24] Sherratt, J.A.: On the evolution of periodic plane waves in reaction-diffusion systems of λ-ω type. SIAM J. Appl. Math. 54, 1374–1385 (1994).

[25] Sherratt, J.A.: Periodic waves in reaction-diffusion models of oscillatory biological systems. FORMA 11, 61-80 (1996).

[26] Sherratt, J.A., Smith, M.J.: Periodic travelling waves in cyclic populations: field studies and reaction-diffusion models. J. Roy. Soc. Interface 5, 483–505 (2008).

[27] Sherratt, J.A., Smith, M.J.: Transition to spatiotemporal chaos via stationary branching shocks and holes. Physica D: Nonlinear Phenomena 241(15), 1671–1679 (2012).

[28] Smith, M.J., Rademacher, J.D.M., Sherratt, J.A.: Absolute stability of wavetrains can explain spatiotemporal dynamics in reaction-diffusion systems of lambda-omega type. SIAM J. Appl. Dyn. Syst. 8, 1136–1159 (2009).

[29] Smith, M.J., Sherratt, J.A.: The effects of unequal diffusion coefficients on periodic travelling waves in oscillatory reaction-diffusion systems. Physica D: Nonlinear Phenomena 236(2), 90–103 (2007).

[30] Smith, M.J., Sherratt, J.A., Lambin, X.: The effects of density-dependent dispersal on the spatiotemporal dynamics of cyclic populations. J. Theor. Biol. 254(2), 264–274 (2008).

[31] Wang, H., Shu, C.W., Zhang, Q., Stability and Error Estimates of Local Discontinuous Galerkin Methods with Implicit-Explicit Time-Marching for Advection-Diffusion Problems, SIAM J. Numer. Anal. 53(1), 206227 (2015).